

150076

ARCHITECTURE OF NEW GENERATION NETWORKS

150016

A THESIS SUBMITTED TO THE GRADUATE SCHOOL OF
NATURAL AND APPLIED SCIENCES
OF
ÇANKAYA UNIVERSITY

BY

ÇAĞLAR ARPALI

IN PARTIAL FULFILLMENT OF THE REQUIREMENTS FOR THE
DEGREE OF MASTER OF SCIENCE
IN
THE DEPARTMENT OF COMPUTER ENGINEERING

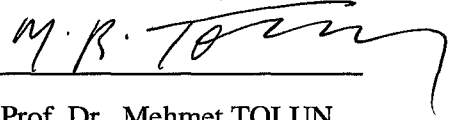
JUNE 2004

Approval of the Graduate School of Natural and Applied Sciences.



Prof. Dr. Yurdahan GÜLER
Director

I certify that this thesis satisfies all the requirements as a thesis for the degree of
Master of Science.



Prof. Dr. Mehmet TOLUN
Chairman Of The Department

This is to certify that we have read this thesis and that in our opinion it is fully
adequate, in scope and quality, as a thesis for the degree of Master of Science.



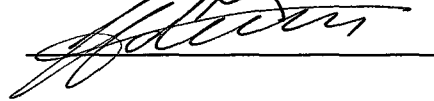
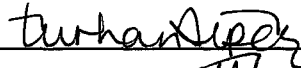
Asst. Prof. Dr. Halil T. EYYUBOĞLU
Supervisor

Examining Committee Members

Prof. Dr. Turhan ALPER

Asst. Prof. Dr. Halil T. EYYUBOĞLU

Dr. Veli Hüsnü TOKMEN



ABSTRACT

Architecture of New Generation Networks

Arpali, Çağlar

Ms, Department of Computer Engineering

Supervisor: Asst. Prof. Dr. Halil T. Eyyuboğlu

June 2004, 64 pages

In this thesis, two macro cell propagation models for network architecture of Universal Mobile Communication System (UMTS), namely, UMTS vehicular ITU-R model [1] and extended Okumura Hata model [2] are compared using digital map and field measured data collected from a particular site in Ankara, Turkey. Comparison is made on the basis of different environment of vegetations, terrains, buildings types and morphology structures. To overcome the inadequacy of the second propagation model, we have proposed different topography and morphology corrections. For this purpose, sample calculations are performed for path lengths of 2700 *m* while the general results are plotted for a range of 6000 *m*. We have also investigated radio network planning with related link budgets for comparing the cell ranges of both models according to the difference service type of 12.2 *kbps* voice and 384 *kbps* real-time data. Our findings indicate that in the determination of signal path loss, average buildings height (Δ_{mr}) is more decisive than others in UMTS vehicular ITU-R model, whereas for extended Okumura Hata model, topographic structure of the terrain (C_d) and effective antenna height (h_{eff}) are most dominant factors and UMTS vehicular ITU-R model predicts shorter cell ranges with respect to extended Okumura model.

Key Words: UMTS, Propagation, Signal Path Loss, Radio Network Planning

ÖZ

Yeni Nesil Ağ Mimarileri

Arpali, Çağlar

Yüksek Lisans, Bilgisayar Mühendisliği

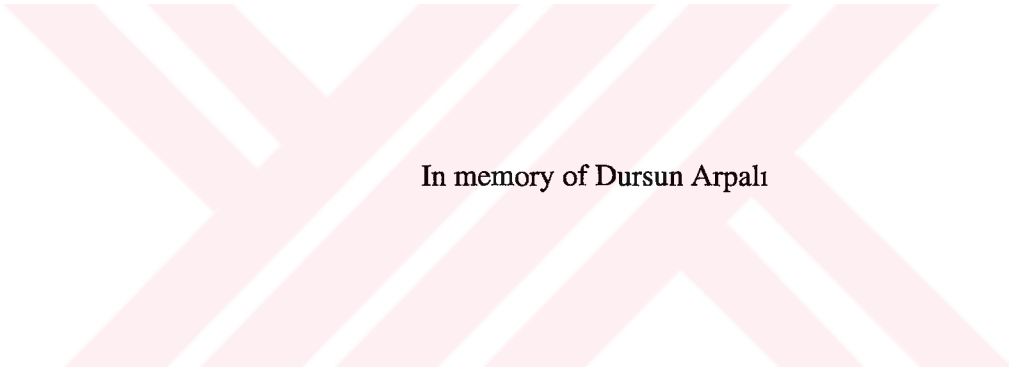
Tez Yöneticisi: Yrd Doç. Dr. Halil T. Eyyuboğlu

Haziran 2004, 64 sayfa

Bu tezde, isimleri UMTS araçsal ITU-R modeli [1] ve genişletilmiş Okumura Hata modeli [2] olan iki büyük hücre yayılım modellerinin, Evrensel Hareketli İletişim Sistemi'nin(UMTS) ağ mimarisi için sayısal harita ve Ankara, Türkiye içinden belli bir alandan toplanan arazi verileri kullanılarak karşılaştırılması yapılmıştır. Karşılaştırma, farklı çevresel bitki örtüleri, araziler, bina yapıları ve coğrafi yapılar temel alınarak yapılmıştır. İkinci yayılım modelinin eksikliğini çözmek için farklı topoğrafik ve coğrafi düzeltmeler önerdik. Bu amaçla, genel sonuçlar 6000 m' lik menzil için çizilirken örnek hesaplamalarda, yol uzunluğunun 2700 m' lik mesafesi için yapıldı. Ayrıca radyo ağ planlaması ile ilişkili olan link bütçelerini her iki modelin hücre menzillerinin farklı servis türleri olan 12.2 kbps ses ve 384 kbps gerçek-zamanlı veri için inceledik. Bulgularımız sinyal yol kaybının bulunmasında, UMTS araçsal ITU-R modeli için ortalama bina yüksekliğinin (A_{mr}), genişletilmiş Okumura Hata modeli içinse arazinin topoğrafik yapısının (C_d) ve etkin anten yüksekliğinin (h_{eff}) diğer faktörlerden daha etkili olduğunu göstermiştir ve UMTS araçsal ITU-R modeli, genişletilmiş Okumura Hata modeline göre daha kısa hücre menzilleri tespit etmiştir.

Anahtar Kelimeler: UMTS, Yayılım, Sinyal Yol Kaybı, Radyo Ağ Planlaması

1



In memory of Dursun Arpalı

ACKNOWLEDGEMENTS

I express sincere appreciation to Asst. Prof. Dr. Halil T. Eyyubođlu for his guidance and insight throughout the research. Then I must thank to Assoc. Prof. Dr. Yahya Baykal for his encouragements. My friends Serap Altay and Barbaros Preveze are gratefully acknowledged. To my parents, I offer sincere thanks for their unshakable faith in me and their willingness to endure with me during my endeavors. I wish to thank to TCK (Türkiye Karayolları Kurumu) for providing helpful discussions on the matter.



TABLE OF CONTENTS

ABSTRACT.....	i
ÖZ.....	ii
ACKNOWLEDGEMENTS.....	iv
TABLE OF CONTENTS.....	v
TABLES.....	viii
FIGURES.....	ix
SYMBOLS.....	x
ABBREVIATIONS.....	xii
CHAPTERS	
CHAPTER 1.....	1
INTRODUCTION.....	1
CHAPTER 2.....	4
PROPAGATON MODELS.....	4
2.1 Modeling Terrains.....	5
2.2 UMTS Vehicular Propagation Model.....	6
2.2.1 Path Loss for UMTS Vehicular Model.....	6
2.3 Extended Okumura Hata Propagation Model.....	8
2.3.1 Path Loss Parameters for Extended Okumura Model.....	10
2.3.1.1 Effective Antenna Height.....	10
2.3.1.2 Morphology Correction.....	12
2.3.1.3 Topographic Corrections.....	13
2.3.1.3.1 Multiple Knife-Edge Diffraction Method.....	13
2.3.1.3.2 Clearance Angle Method.....	17
CHAPTER 3.....	20
RADIO NETWORK PLANNING.....	20

3.1 Radio Link Budget and Cell Range Calculation.....	20
CHAPTER 4	31
SAMPLE CALCULATIONS FOR PROPAGATION MODELS	31
4.1 Preliminary Assumptions	31
4.2 Path Loss Calculations	33
4.2.1 Path Loss Calculation for Extended Okumura Model.....	33
4.2.1.1 Effective Antenna Height Calculation	33
4.2.1.2 Morphology Correction Factor Calculation	34
4.2.1.3 Topography Corrections Factor Calculation	34
4.2.1.4 Path Loss Calculation for Sector 1 Using Multiple Knife-Edge Diffraction Method	35
4.2.1.5 Path Loss Calculation for Sector 2 Using Clearance Angle Method.....	37
4.2.1.6 Path Loss Calculation for Sector 3 Using Clearance Angle Method.....	38
4.2.2 Path Loss Calculation for UMTS Vehicular Model	39
4.3 Results of Simulation Program	40
4.3.1 Sector 1.....	42
4.3.1 Sector 2.....	43
4.3.1 Sector 3	44
CHAPTER 5	47
RADIO LINK BUDGET CALCULATION.....	47
5.1 Radio Link Budget Calculation	47
5.2 Cell Range Calculation.....	56

CHAPTER 6	61
CONCLUSIONS	61
REFERENCES	63



LIST OF TABLES

TABLES

3.1: Required parameters for radio link budget	21
4.1: Measured results for UMTS vehicular model	40
4.2: Path loss results for 2700 m	40
5.1: Link budget of 12.2 kbps voice service	54
5.2: Link budget of 384 kbps real-time data service	55
5.3: Cell ranges with respect to service type.....	57

LIST OF FIGURES

FIGURES

2.1: Terrain profile of UMTS vehicular model.....	7
2.2: Effective antenna height	12
2.3: Sample morphology correction	13
2.4: Terrain height profile for Sector 1.....	14
2.5: Diffraction path profiles for Sector 1.....	16
4.1: Terrain height profile for Sector 2.....	37
4.2: Terrain height profile for Sector 3.....	39
4.3: Path losses versus distance for Sector 1.....	43
4.4: Path losses versus distance for Sector 2.....	44
4.5: Path losses versus distance for Sector 3.....	45
5.1: Cell structures for 12.2 <i>kbps</i> voice	59
5.2: Cell structures for 384 <i>kbps</i> real-time data	59

SYMBOLS

Δd	:	Correction Factor Due To Clearance Angle
$c(h_r)$:	Correction Function For Mobile Height
C_d	:	Topography Correction Factor
C_m	:	Morphology Correction Factor
d	:	Distance From Base Station To Mobile
E_b/N_o	:	Signal To Noise Ratio
F	:	Receiver Noise Figure
f	:	Carrier Frequency
h_{eff}	:	Effective Height Of The Transmitter
h_m	:	Average Height Of The Terrain
h_n	:	Physical Height Of The Antenna Above Sea Level
h_r	:	Mobile Station Antenna Height
H_t	:	Base Station Antenna Height
L	:	Total Average Path Loss
ℓ	:	Average Separation Between The Buildings
N_o	:	Thermal Noise Density
PG	:	Processing Gain
P_{NP}	:	Total Effective Noise Power

- P_{rx} : Receiver Interference Power
- r : Radial Distance From Rooftop To Mobile Station
- x : Horizontal Distance Between The Mobile And The Diffracting Edge
- Δ_{hb} : Difference Between The Base Station Antenna Height And Mean Building Roof Top Height
- Δ_{hm} : Difference Between The Mean Building Height And Mobile Station Antenna Height
- Δ_m : Mean Building Rooftop Height
- Δ_{mr} : Mean Building Height
- η : Interference Margin
- Θ : Angle Subtended At The Mobile Station Form The Diffraction Point

LIST OF ABBREVIATIONS

UMTS	:	Universal Mobile Communication System
ITU	:	International Telecommunication Union
COST	:	European Cooperation Of Scientific And Technical Research
VHF	:	Very High Frequency
UHF	:	Ultra High Frequency
CCIR	:	Centre for Communication Interface Research
EBU	:	European Broadcasting Union
ETSI	:	European Telecommunications Standards Institute
WCDMA	:	Wideband Code Division Multiple Access
3GPP	:	3 rd Generations Partnership Project
BLER	:	Block Error Rate

CHAPTER 1

INTRODUCTION

To implement a mobile radio system, wave propagation models are necessary to determine the propagation characteristics for site installations. Propagation models are used to predict the signal field strength of a given transmitter in the computation area. Because of different obstacles and complex scattering structures in the radio channel, it is impossible to construct exact models; therefore accurate approximate models are required. In third generation mobile systems, UMTS, this process includes the prediction of the received power, delay spread, angular spread and impulse response of the mobile radio channel in order to determine the parameter sets of the base stations. The environments where these systems are intended to be installed vary from indoor up to large rural areas. Hence wave propagation prediction methods and scenarios are required covering the whole range of macro, micro and pico cells. In macro cell configurations, semi-empirical models based on UMTS vehicular ITU-R (hereafter referred to as UMTS vehicular) and extended Okumura Hata (hereafter referred to as extended Okumura) models can be used. Due to several years of experience, these models combine short computation times with the high accuracy of a deterministic approach. Multipath phenomenon characterizes the radio wave propagation within urban and suburban environments.

The shadowing by buildings or hills gives rise to slow fading. Since the short-term fading of the received signal is almost impossible to predict, all propagation models account for such effects by estimating either the average or median values. With the knowledge of propagation losses, one can efficiently determine the field signal strength, signal-to-noise ratio and carrier-to-interference ratio, etc. Radio propagation prediction is also one of the fundamentals for radio network planning that affects cell range of base station according to selected propagation model. In the dimensioning phase of radio network planning number of base station sites, base stations and their configurations and other network elements (such as cables losses, antenna gains etc.) are estimated based on the requirements and the radio propagation in that area. To calculate link budget of a UMTS network in radio network planning is mostly depended to selected propagation model. In the first part of thesis, our aim is to investigate the validity of both models for a base station having conflicting terrain structures on its isolated sectors and in the second part we have made radio link budget calculations comparing signal path loss models for specific types of services such as 12.2 *kbps* voice and 384 *kbps* real-time data with respect to their cell ranges. To this end, in Sector 1 (in the direction of east) there is dense urbanization with closely spaced tall buildings. Furthermore high terrains exist in this area. Morphology type of Sector 2 (in the direction of northwest) tends towards parks and open areas, with less terrain and building heights. Sector 3 (in the direction of southwest) has a suburban morphology type where there are buildings and terrains of medium height. In this sense, Sector 3 represents a mixture of the Sectors 1 and 2. The remainder of this thesis is organized as follows; In Chapter 2,

we describe the macro cell propagation models (UMTS vehicular and extended Okumura models) and calculation methods. In Chapter 3 radio network planning concepts and radio link budget calculation methods are described. Chapter 4 presents some sample calculations with additional correction factors for topography, morphology where also it summarizes the simulation results in form of graphics for different sectors and also a comparison of the two propagation models are made and the accompanying results are discussed. In Chapter 5 radio link budget calculation, are made and comparing specific types of services such as 12.2 *kbps* voice and 384 *kbps* real-time data with respect to their cell ranges based on the results of Chapter 4. Finally we end with conclusions in Chapter 6.

CHAPTER 2

PROPAGATION MODELS

A propagation model is a combination of mathematical expressions to represent the radio characteristics of a given environment. This prediction model is divided into two main parts. First is based on empirical models while the second is related to deterministic parts. The empirical models are derived from field measurements, whereas the deterministic models deal with the fundamental principles of radio wave propagation phenomena. In the empirical models, all environmental influences are implicitly taken into account regardless of whether they can be separately recognized. The deterministic models work according to principles of physics and, due to that; they can be applied to different environments without affecting the accuracy. Further, in respect of the size of the coverage area, the outdoor propagation models can be subdivided into two additional classes, macro cell and micro cell prediction models. The radio propagation environment is called macro cellular when the base station antenna array is above the average rooftop level. The propagation environment is called micro cellular when the base station antenna array is placed below the average rooftop level. Depending on the type, size and the density of constructions and natural objects, propagation environment

is divided into three main categories; urban, suburban and rural. For macro and micro cells, the line of sight conditions are hardly satisfied; hence diffractions and reflections from buildings are bound to occur. The prediction process is further complicated because the distance from transmitter to receiver varies appreciably, from a few hundred meters to 30000 *m*. In such a situation, the propagation of the waves is of a more statistical nature hence a pure empirical or semi-empirical model is more appropriate. Usually these models use free parameters and different correction factors that can be tuned by using field measurements.

2.1 Modeling Terrains

For the practical prediction of propagation in a real environment, terrains must be described by approximations. This requires a modeling process in which the real terrain has to be digitized yielding digital terrain data. Therefore part of the COST 231 project [3] has focused on the types, resolution and accuracy of digital terrain databases required for propagation modeling. The information includes terrain height, land usage data, building shape and height. In the first step, propagation environment has to be digitized yielding a database, which describes the considered environment in an adequate way. The second step includes the definition of mathematical approximations for the physical obstruction. Data consist of binary stored pixel data with an arbitrary resolution, in our case 30*m* x 30*m*. The different morphological properties urban, suburban, forest, waters, open, etc are also embedded into the same database in coded form.

2.2 UMTS Vehicular Propagation Model

This multipath propagation model being derived from COST 231 outdoor model is adopted by ITU [1] and is applicable for the test scenarios in urban and suburban areas outside the high rise core. The vehicular environment is characterized by large macrocells and large transmit powers. Instead of constructing propagation models for all possible UMTS operating environments, a smaller set of test environments is defined which adequately span the overall range of possible environments. Note that despite the name ‘vehicular’ these models may nothing directly to do with vehicles.

2.2.1 Path Loss for UMTS Vehicular Model

Here the base station antenna is located above the average rooftop, consequently conditions of none line-of-sight for mobile station are satisfied. Therefore we may use UMTS vehicular model for all sectors. In this case, wave propagation is determined by diffraction and reflection at buildings. The geometry is illustrated in Figure 2.1 for a distance of 2700 m from the base station. For UMTS vehicular method, the path loss [1] is expressed with the following equation.

$$L = -10 \log_{10} \left(\frac{\lambda}{4\pi d} \right)^2 - 10 \log_{10} \left[\frac{\lambda}{2\pi^2 r} \left(\frac{1}{\theta} - \frac{1}{2\pi + \theta} \right)^2 \right] - 10 \log_{10} \left[(2.35)^2 \left(\frac{A_{hb}}{d} \sqrt{\frac{\ell}{\lambda}} \right)^{1.8} \right] \quad (2.1)$$

As also partially apparent from the figure 2.1;

H_t is base station antenna height (in m)

d is distance from base station to mobile (in m)

Δ_m is mean building rooftop height (in m)

$\Delta_{hb} = H_t - \Delta_m$ is difference between the base station antenna height and mean building roof top height (in m)

$\Delta_{hm} = \Delta_{mr} - h_r$ is difference between the mean building height and mobile station antenna height (in m)

x is horizontal distance between the mobile and the diffracting edge (in m)

ℓ is average separation between the buildings (in m)

h_r is mobile station antenna height (in m),

Δ_{mr} is mean building height (in m)

θ is the angle subtended at the mobile station form the diffraction point (in $degree$)

r is radial distance from rooftop to mobile station (in m)

L is total average path loss (in dB)

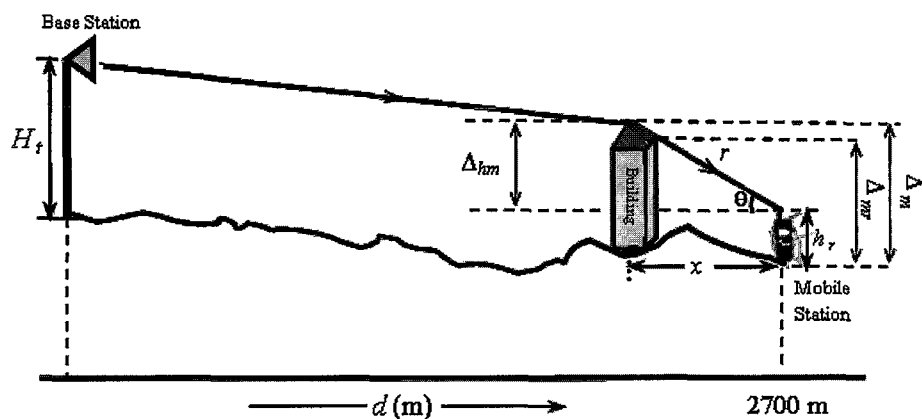


Figure 2.1: Terrain profile of UMTS vehicular model

2.3 Extended Okumura Hata Propagation Model

Extended Okumura model [2] is a simple empirical approach for the prediction in macro cellular areas based on the evaluation of intensive measurements at frequencies between 200 MHz and 2000 MHz with vertical polarization. But for urban personal mobile communication applications such as UMTS at 1500-2000 MHz, it was found by the European study committee COST 231[3] that the Okumura's model consistently underestimates signal path loss; hence its "extended" version was developed to rectify the situation. The field measurements are analyzed statistically and compiled into diagrams. The correction factor for either an open area or a suburban area should be taken into account, such as morphology type, general slope of terrain etc., making the path loss prediction closer to the actual values. The basic formula for the median propagation loss in dB with different correction terms according to different propagation environments (dense, urban, suburban and open) given by extended Okumura propagation loss model is [2]

$$L = 46.3 + 33.9 \log_{10}(f) - 13.82 \log_{10}(h_{eff}) - c(h_r) + (44.9 - 6.55 \log_{10}(h_{eff})) \log_{10}(d) - C_m \quad (2.2)$$

Where

d is distance between transmitter and receiver (in m)

C_m is morphology correction factor (in dB)

$c(h_r)$ is correction function for mobile height (in dB)

h_{eff} is effective height of the transmitter (in m)

h_r is height of the mobile (in m)

f is carrier frequency (in MHz)

L is total average path loss (in dB)

This formula describes the wave propagation in straight forward manner, so we need to adjust C_m depending on our own morphology. There is also a terrain correction factor for extended Okumura model, but it is restricted to generally assumed terrain shapes. In this thesis we have proposed a different morphology correction scheme according to the terrain profile from the map of real morphologic data, and we also add a topographic correction factor to the main propagation loss.

As a result, the equation 2 becomes;

$$L = 46.3 + 33.9 \log_{10}(f) - 13.82 \log_{10}(h_{eff}) - c(h_r) + (44.9 - 6.55 \log_{10}(h_{eff})) \log_{10}(d) - C_m + C_d \quad (2.3)$$

Where

$$c(h_r) = (1.1 \log_{10}(f) - 0.7) \times (h_r) - (1.56 \log_{10}(f) - 0.8) \quad (2.4)$$

In this formula, C_d is the added topography correction factor in dB . The ranges of the parameters for which this model is considered valid are listed below;

$$1500 \leq f (MHz) \leq 2000 \quad 30 \leq h_{eff}(m) \leq 200$$

$$1000 \leq d (m) \leq 10000 \quad 1 \leq h_r (m) \leq 10$$

Vertical line on the left side of the page.



This is a method originally developed for VHF and UHF land-mobile radio systems involving complex computation. Most of its experimental data have been incorporated into the ITU (CCIR) reference curves. In order to make the Okumura technique suitable for computer simulation, the analytic expressions for the medium path loss for urban, suburban and open areas were developed. Still these expressions are only approximations therefore having some limitations. Hence we have used calculated values with real measured data instead of the basic Okumura curves. In extended Okumura model, propagation prediction includes multiple diffractions over terrains and buildings. But when the base station is located above the surroundings obstacles in order to cover a large area, scattering and reflection from hills, mountains and buildings are neglected in Okumura model consequently in our calculations as well.

2.3.1 Path Loss Parameters for Extended Okumura Model

The parameters affecting the path loss for Extended Okumura Model can be classified into three sub parts; effective antenna height, morphology correction and topographic correction.

2.3.1.1 Effective Antenna Height

In propagation calculations, the definition of the correct antenna height may substantially improve the accuracy of the results. There are several methods to define the effective antenna height of a base station. If the terrain is flat, then the effective antenna height is the same as the physical antenna height from the ground. However, if the terrain is undulating, the selection of the calculation method may

have an impact on the results. In this thesis, we have used the method suggested by CCIR [4]. There the effective height of an antenna h_{eff} , is defined as the height above the average terrain level in the range from the starting point (base station antenna) to the end point (mobile station). Hence h_{eff} may be calculated as follows [4];

$$h_{eff} = h_n - h_m \quad (2.5)$$

Where,

h_n is physical height of the antenna above sea level (in m)

h_m is average height of the terrain (in m)

The average height of the terrain h_m is calculated from the following equation,

$$h_m = \frac{\sum_{i=0}^n h_i}{n + 1} \quad (2.6)$$

h_i is the heights from the starting point to the end point

Figure 2.2 illustrates the calculation method of effective antenna height h_{eff} for general terrain profile.

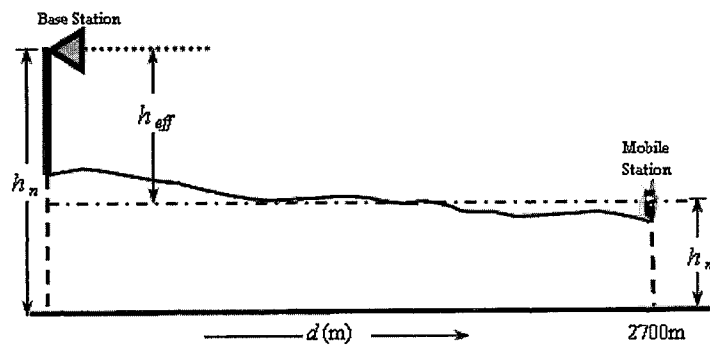


Figure 2.2: Effective antenna height

2.3.1.2 Morphology Correction

The correction due to morphology is the best-known correction method for the common propagation models. The result of the basic propagation model is adjusted according to the terrain types between the mobile station and the base station. Figure 3 demonstrates how we calculate the morphology correction. In this figure, distance between the base station and the mobile station is assumed to be 660 m, and calculations are made accordingly. As indicated in Figure 2.3, each pixel representing a terrain type within the 30 m x 30 m area is denoted by a different notation such as U = urban, S = suburban, P = park, O = open, W = water, F = forest. Related correction factors of these terrain types are placed immediately underneath the terrain type in the same figure. The morphology correction is calculated as an average of the pixels between the mobile station and the base station. Average of the correction factors for the example in given in Figure 3 is -9.6 dB. But it is not very likely that the area close to the base station has a great impact on the received power of the mobile station, so the terrain type pixels are assigned ascending weights towards the receiver side. These weights are in the

range 1.0 to 2.0. These are then converted into (in the fourth line of Figure 2.3) normalized weights upon dividing by their average. Eventually normalized correction factor is obtained by the multiplication of second and fourth lines. For the example given, the average normalized correction factor (at a distance of 660 m) is -10.6 dB.

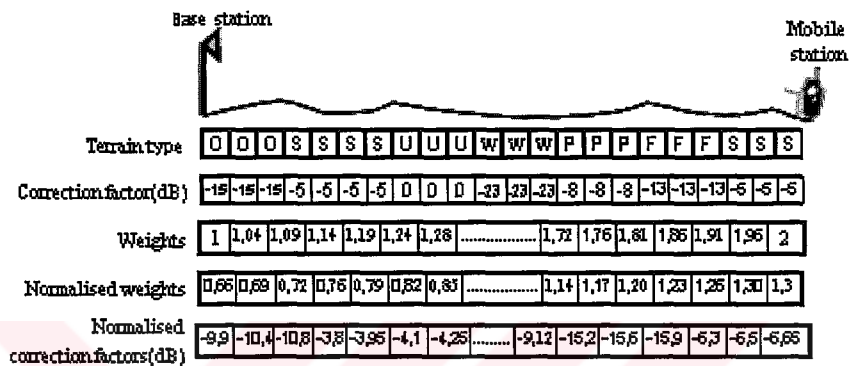


Figure 2.3: Sample morphology correction

2.3.1.3 Topographic Corrections

Topographic corrections in coverage predictions are usually made with the help of the terrain height model. These are based on field strength measurements and statistical processing. According to terrain structure there are suitable topographic correction methods. In generally usages, most known ones were multiple knife-edge diffraction method and clearance angle method.

2.3.1.3.1 Multiple Knife-Edge Diffraction Method

Diffraction occurs when the direct line-of-sight propagation between the transmitter and the receiver is obstructed by an opaque obstacle whose dimensions are considerably larger than the signal wavelength. Diffraction loss for an ideal knife-

edge obstruction can be calculated from the famous Fresnel integral. In application to radio propagation, formulas based on this integral have frequently provided close approximations to the diffraction effects of isolated mountain ridges. Deygout [5] provides easily implemented procedures for calculation when the terrain can be represented this way. The technique described in this thesis involves multiple knife-edge configurations for Sector 1.

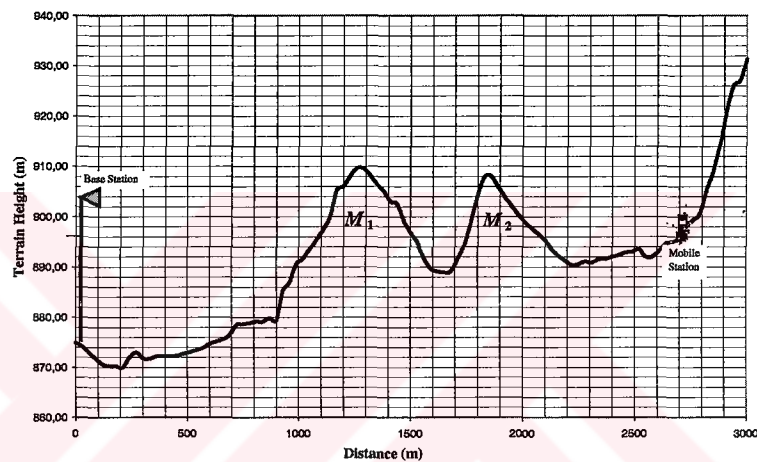


Figure 2.4: Terrain height profile for Sector 1

General profile for Sector 1 is shown in Figures 2.4 and 2.5. As seen from these figures, within a distance of 2000 m, terrain shapes include two main irregular and knife-edge hills named as M_1 and M_2 respectively. Further on, there is another obstacle located around 3000 m, from there onwards; the topography becomes nearly flat for the rest of the path, though not shown explicitly in Figure 2.4. So the simulation program is adjusted to take into account these three obstacles at the given distances. To calculate the diffraction loss, the main diffraction paths have to

be defined from transmitter to receiver. The cross section path profile from base station to mobile is given in Figure 2.5.

In this figure;

H_t is height of the transmitter above the straight line d , joining the transmitter and the receiver (in m)

H_r is height of the receiver above the straight line d , joining the transmitter and the receiver (in m)

H_{m1} is height of the terrain M_1 from the path line d (in m)

H_{m2} is height of the terrain M_2 from the path line d (in m)

d is distance between transmitter and receiver (in m)

x is distance between transmitter and receiver through the direct path joining the two ends (in m)

M_1 is first obstacle

M_2 is second obstacle

h_1 is height of the top of the obstacle M_1 above the straight line x joining the two ends of the paths (in m)

h_2 is height of the top of the obstacle M_2 above the second diffraction path (in m)

h_3 is height of the top of the obstacle M_2 above the straight line x joining the two ends of paths (in m)

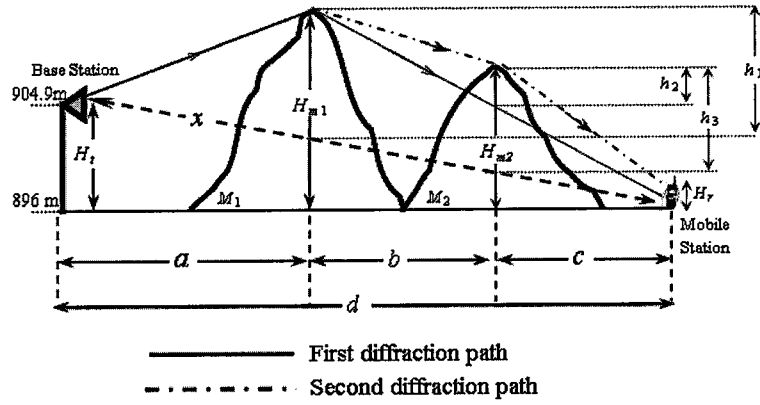


Figure 2.5: Diffraction path profiles for Sector 1

Numeric values of the parameters h_1 , h_2 and h_3 given in Figure 2.5 may be calculated from the following equations [6];

$$h_1 = H_{m1} - \left(H_t + \left(\frac{H_r - H_t}{a+b+c} \right) \times a \right), \quad (2.7)$$

$$h_2 = h_3 - h_1 \times \left(\frac{c}{b+c} \right) \quad (2.8)$$

$$h_3 = H_{m2} - \left(H_t + \left(\frac{H_r - H_t}{a+b+c} \right) \times (a+b) \right) \quad (2.9)$$

In the topographical structure of Sector 1, one edge (obstacle M_1) is predominant in the terrain. The first diffraction path is defined by the distances a and $b+c$ and the height h_1 . The second diffraction path is defined by the distances b and c and the height h_2 . In order to calculate the received field strength, the diffraction losses are added to main propagation loss. To this end, we have named the diffraction loss due to the main obstacle M_1 as A_{m1} and the diffraction loss due to the secondary obstacle

M_2 as A_{m2} . The first path values a , $b+c$ and h_1 are used to determine v_{m1} in accordance with equations 2.10, 2.11 and 2.12. The values b , c and h_2 are to be used for calculation of v_{m2} . For obstacles M_1 and M_2 diffraction loss is calculated from the following equations [6];

$$A = 6.4 + 20 \log_{10} \left(\sqrt{v^2 + 1} + v \right) \quad (2.10)$$

$$v_{m1} = h_1 \times \sqrt{\frac{2}{\lambda} \times \left(\frac{1}{a} + \frac{1}{(b+c)} \right)} \quad (2.11)$$

$$v_{m2} = h_2 \times \sqrt{\frac{2}{\lambda} \times \left(\frac{1}{c} + \frac{1}{b} \right)} \quad (2.12)$$

Where

$A = A_{m1}$, $v = v_{m1}$ for obstacle M_1 and

$A = A_{m2}$, $v = v_{m2}$ for obstacle M_2 .

Then the total topographic diffraction loss, C_d due to obstacles M_2 and M_1 is found as;

$$C_d = A_{m1} + A_{m2} \quad (2.13)$$

2.3.1.3.2 Clearance Angle Method

Clearance angle method achieves quite remarkable prediction accuracy for path loss calculation on macro cells. Clearance angle method may be useful for topographic correction in cases where for example diffraction method is not working well. The clearance angle method is first proposed by the European Broadcasting Union

(EBU) [7] and later adopted by CCIR [8]. The angle, φ is measured relative to the line from the receiving antenna which just clears all terrain obstructions in the direction of the transmitter antenna as depicted later in Figures 4.1 and 4.2. Topographic correction factor in terms of the clearance angle is given in the form of two curves, one for VHF and the other for the UHF band. UMTS operates around 2000 MHz. Hence in our calculations we have adopted the figures of UHF band. The relevant correction factor should be added to the field strength level obtained from the CCIR reference curves supplied in Ref. 10. In our situation, distance between the base station and the mobile station varies from 0 to 6000 m, so we have not taken into consideration the CCIR reference curves, but have used the actual calculated clearance angle values where there is a separation of 2700 m between the base station and the mobile station. The clearance angle can be determined for a maximum distance of 16000 m. But in our measurements, the distance between the base station and the mobile station is less. So the clearance angle correction factor for UHF band will be given by the following equations [6];

$$\Omega = -93.095 \times \varphi, \quad \Delta d = 14.9 - \left[6.9 + 20 \log_{10} \left(\sqrt{(\Omega - 0.1)^2 + \Omega - 0.1} \right) \right] \quad (2.14)$$

$$C_d = \frac{\Delta d \times d(km)}{16(km)} \quad (2.15)$$

Where

C_d is topographic correction factor due to clearance angle (in dB)

Δd is correction factor due to clearance angle calculated for a given distance between transmitter and receiver (in dB)

d is distance between the base station and the mobile station (in km).



CHAPTER 3

RADIO NETWORK PLANNING

The UMTS radio network planning process consists of two parts; dimensioning (initial planning) and detailed radio network planning. Each part requires additional support functions, such as propagation measurements, base station configuration and so on. Dimensioning is the first phase of planning and its purpose is to initially draft the radio network configuration and deployment strategy for long-term. In detailed radio network planning; coverage, capacity and frequency planning have to be done and documented. Dimensioning includes some parameters such as traffic and coverage threshold. They have a strong influence on coverage, capacity and quality in the radio network and related to base station antenna heights in the radio network. Initial planning also includes radio link budget (power budget). In order calculated coverage and cell ranges are utilized in the link budget calculation.

3.1 Radio Link Budget and Cell Range Calculation

To estimate the maximum range of a cell, a radio link budget is needed. In the link budget, the antenna gains, cable losses, fading margin, etc., are taken into account. The output of the link budget calculation is the maximum allowed propagation path loss, which in return determines the cell range with respect to a specific service type

such as 12.2 *kbps* voice or 384 *kbps* real-time data. To convert path loss to the cell range, a known radio propagation model can be used such as Okumura or UMTS vehicular models. In order to calculate the maximum allowed path loss between the base station and the mobile station and to select the optimized base station site configuration, all these parameters have to be collated in the radio link budget. General structure of link budget calculation and required parameters [9] are given in the Table 3.1. Now we investigate these parameters in details.

Table 3.1: Required parameters for radio link budget

Transmitter (mobile)	
(a)	Maximum transmitter power (in <i>dBm</i>)
(b)	Mobile antenna gain (in <i>dB</i>)
(c)	Cable, connector and body loss (in <i>dB</i>)
(d)	Transmitter equivalent isotropic radiated power (in <i>dBm</i>)
Receiver (base station)	
(e)	Thermal noise density, N_o (in <i>dBm/Hz</i>)
(f)	Receiver noise figure, F (in <i>dB</i>)
(g)	Receiver noise density (in <i>dBm/Hz</i>)
(h)	Receiver noise power, P_n (in <i>dBm</i>)
(i)	Interference margin, η (in <i>dB</i>)
(j)	Receiver interference power, P_{rx} (in <i>dBm</i>)
(k)	Total effective noise power, P_{NP} (in <i>dBm</i>)
(l)	Processing gain, PG (in <i>dB</i>)
(m)	Required E_b/N_o (in <i>dB</i>)
(n)	Receiver sensitivity (in <i>dBm</i>)
(o)	Receiver antenna gain (in <i>dB</i>)
(p)	Cable and connector losses (in <i>dB</i>)
(r)	Maximum path loss (in <i>dB</i>)
(s)	Log-normal fade margin (in <i>dB</i>)
(t)	In-car loss (in <i>dB</i>)
(u)	Allowed propagation loss for cell range (in <i>dB</i>)

(a) Maximum Transmitter Power

Maximum transmitter power is defined as the total power at the transmitter output for a single traffic channel. A traffic channel is defined as a communication path between a mobile station and a base station used for user and signaling traffic. The term traffic channels imply a forward traffic channel and reverse traffic channel pair. European Telecommunications Standards Institute (ETSI) has defined four power classes for mobile hand set [9] and for radio link budget it is recommended that $0.125 \text{ W} = (21 \text{ dBm}^1, \text{ class 2})$, power for voice transmission and $0.25 \text{ W} = (24 \text{ dBm}, \text{ class 3})$ power for real-time data services will be suitable. In our radio link budget calculations, we have used these two power classes for mobile hand sets.

(b) Mobile Antenna Gain (Transmitter)

Transmitter antenna gain is the maximum gain of the transmitter antenna in the horizontal plane (specified as dB relative to an isotropic radiator).

(c) Cable, Connector, and Body Losses (Transmitter)

These are the combined losses of all transmission system components between the transmitter output and the antenna input plus body of mobile user (all losses in positive dB values). For mobile station, cable and connector losses are very small so the body loss has a greater impact than the other losses and the measured value is approximately 3 dB and assumed as constant in the radio link budget.

1. The Unit dBm measure the power or voltage received by an antenna in the field. This unit measure received energy level and defined as $\text{dBm} = 10 \log_{10} \left(\frac{P}{1 \text{ mW}} \right)$, where P is power measured at the receiver.

(d) Transmitter Equivalent Isotropic Radiated Power (e.i.r.p.)

This is the summation the total transmitter power and the transmitter antenna gain minus transmission system losses, in the direction of maximum radiation to be given by the following equation [10] (i.e. row (d) from Table 3.1);

$$d = a + b - c \quad (3.1)$$

(e) Thermal Noise Density (N_o)

Thermal noise density, N_o , is defined as the noise floor due to thermal noise per hertz at the receiver input. It is provided the following equation [11]:

$$N_o = k \times T \quad (3.2)$$

Where

N_o is thermal noise density (in dBm / Hz)

k is Boltzman's constant (in $Ws/Kelvin$)

T is outside temperature of receiver (in $Kelvin$)

(f) Receiver Noise Figure (F)

Receiver noise figure is the noise figure of the receiving system referenced to the receiver input. The receiver noise figure is also commonly expressed as noise temperature of receiver (T_o) divided by outside temperature of receiver (T) which is given by equation 3.3 [12];

$$F = 10 \log_{10} \left(1 + \frac{T_o}{T} \right) dB \quad (3.3)$$

Where

T_o is noise temperature of receiver (in *Kelvin*)

T is outside temperature of receiver (in *Kelvin*)

F is noise figure of the receiver (in *dB*)

T_o depends on the type of antenna employed for base station

(g) Receiver Noise Density

When the receiver noise figure (F) is added to thermal noise density (N_o), the resultant is called the receiver noise density (it defines the noise density at the receiver) and calculated with the following equation in radio link budget [10] as row (g).

$$g = e + f \quad (3.4)$$

(h) Receiver Noise Power

Noise power defines the noise power at the receiver within the channel bandwidth of the receiver [13] and given with the following equation:

$$P_n = k \times T \times B \times F \quad \text{where} \quad (3.5)$$

P_n is noise power (in *dBm*)

k is Boltzman's constant (in *Ws/Kelvin*)

T is outside temperature of receiver (in *Kelvin*)

F is noise figure of the receiver (in *dB*)

B is chip rate (in Mhz)

The value of B is constant for UMTS and equal to $3.84 Mhz$ and also defines the effective bandwidth of the system

(i) Interference Margin

UMTS uses Wideband Code Division Multiple Access (WCDMA) as air interface access technique. In WCDMA there is interference from the original cell and from the neighboring cells. The degradation of coverage and capacity is modeled with an interference margin. This depends on load as shown in the following equation [13]

$$\eta = -10 \log_{10}(1 - load) \quad (3.6)$$

where η is interference margin (in dB)

The load is always compared to the maximum capacity of the cell (called pole capacity) so the load is always in between 0 percent and 100 percent.

(j) Receiver Interference Power

Receiver interference power describes the noise level at the receiver due to interference i.e. without thermal noise. The calculation is done by subtracting Noise power (P_n) from the sum of Noise power and Interference margin (η). Calculation is done by using the absolute values and calculated the following equation: [11]

$$P_{RX} = (P_n + \eta) - P_n = 10^{(P_n + \eta)/10} - 10^{P_n/10} \quad (3.7)$$

Where P_{RX} is receiver interference power (in dBm)

(k) Total Effective Noise Power

Total effective noise is the noise floor including thermal noise, noise generated by the receiver (noise figure) and interference. Total noise power is calculated to be Receiver noise power plus Receiver interference power and given with the following equation [11]:

$$P_{NP} = (P_n + P_{RX}) = 10^{(P_n/10)} + 10^{(P_{RX}/10)} \quad (3.8)$$

Where P_{NP} is total effective noise power (in *dBm*)

(l) Processing Gain

Processing gain is a gain that is achieved due to spreading and depends on data bit rate of service type. The gain can be calculated with the following equation [11]:

$$PG = 10 \log_{10} \left(\frac{B}{W} \right) \quad (3.9)$$

B is chip rate (in *Mcps*)

PG is processing gain (in *dB*)

W is the bit rate of the information (in *Mcps*)

The value of B is constant for UMTS and can be defined in terms of *Mcps* unit which equals to 3.84 *Mcps*.

(m) Required E_b/N_o

The E_b/N_o that is needed to be able to demodulate the signal shows ratio between the received energy per bit and noise energy. E_b/N_o requirement depends on the bit

rate, service, multipath profile, mobile speed and receiver algorithms. The value should be selected based on the service from the 3rd Generations Partnership Project (3GPP) performance requirements [14]. The performance indicator E_b/N_o is always related to some quality Block Error Rate (BLER) target. BLER is long term average block error rate calculated for the transport blocks. The transport block is considered erroneous if it has at least one bit error.

(n) Receiver Sensitivity (Base Station)

This is the signal level needed at the receiver to be able to achieve acceptable quality input that satisfies the required E_b/N_o , and given by the following equation [10] (i.e. row (n) from Table 3.1);

$$n = m - l + k \tag{3.10}$$

(o) Receiver Antenna Gain (Base Station)

Receiver antenna gain is the maximum gain of the receiver antenna in the horizontal plane (specified as dB relative to an isotropic radiator) and depends on the type of antenna employed for base station.

(p) Cable, Connector Losses (Receiver)

These are the combined losses of all transmission system components between the receiving antenna output and the receiver input (all losses in positive dB values).

(r) Maximum Path Loss

This is the maximum loss that permits required performance at the cell boundary and given the following equation [10] (i.e. row (r) from Table 3.1);

$$r = d - n + o - p \tag{3.11}$$

(s) Log-Normal Fade Margin

The log-normal fade margin is defined at the cell boundary for isolated cells. This is the margin required to provide specified coverage availability over the individual cells. Log-normal fading, often called shadowing, is caused by the mobile moving into the shadow of hills, trees or buildings. According to various measurements the mean path loss closely follows a log-normal distribution. When planning coverage for a mobile network, one quality target is location probability of coverage. This means that field strength must be better than the given threshold with some probability. This is defined as outage probability and given by the following Gaussian distribution equation [15];

$$P_{out} = \Pr(x > \rho) = \frac{1}{\sqrt{2\pi}\sigma} \int_{\rho}^{\infty} e^{-x^2/2\sigma^2} dx = Q\left(\frac{\rho}{\sigma}\right) \tag{3.12}$$

As x has a Gaussian distribution in dB, the integral of Gaussian distribution is expressed in terms of the Q function that is given with the following equation;

$$Q(x) = \int_x^{\infty} \frac{1}{\sqrt{2\pi}} e^{-\frac{t^2}{2}} dt \tag{3.13}$$

(t) In-Car Loss

To guarantee coverage for vehicular environment, additional margin is needed due to loss of in-car user. According to measurements, the matter loss of a car approximately is 4-7 *dB*. So in our link budget, we have assumed in-car loss as 4 *dB* for both services (voice and real-time data).

(u) Allowed Propagation Loss For Cell Range

This loss is used in calculation of cell range and includes max path loss and other losses such as in-car loss and log-normal fading margin then maximum range is computed for each service deployment scenario according that loss. Defining with the following equation [16] (i.e. as row (*u*) from Table 3.1);

$$u = r - s - t, \quad (3.14)$$

3.2 Maximum Range

Maximum range, R_{max} is given by the range associated with the maximum allowed propagation path loss. From the link budget, the cell range can be calculated for a known propagation model, for example extended Okumura model or UMTS vehicular model. The propagation model describes the average signal propagation in that environment, and it converts the maximum allowed propagation loss in *dB* on the link budget Table 3.1 as field's row (*u*) to the maximum cell range in kilometers. After calculating the cell range from propagation model, then the coverage area can be estimated from the following equation [13];

$$S = K.d^2 \quad (3.15)$$

Where S is the coverage area, d is the maximum cell range and K is the constant depending on type of sectorization used for cell site (for 3-sectored case, $K = 1.95$) [13]. In case of hexagonal deployment of sectored cells, the radius of a hexagon shaped cell is defined as [10];

$$D = \sqrt{\frac{2 \times K \times d^2}{3\sqrt{3}}} \quad (3.16)$$

Where D is the radius of hexagonal shaped cell, d is the maximum cell range and K is the constant



CHAPTER 4

SAMPLE CALCULATIONS FOR PROPAGATION MODELS

4.1 Preliminary Assumptions

We have analyzed an extensive amount of data collected in a large number of existing macro cells. The experimental data were taken from a particular site in the city of Ankara for the range of 0-6000 *m* with 30 *m* intervals (using a digital map with a resolution of 30 x 30) to calculate path losses for corresponded sectors. The simulation programs, written in Matlab, incorporate the actual field data of each sector for 6000 *m* distances from the base station. The base antenna height is set to 30 *m*, which is above the surrounding average measured building height for all sectors. The mobile antenna height is 1.5 *m* within all sectors. In the first part (Chapter 4) of the thesis; the losses and gains arising from the base station and mobile station antennas and its equipments such as cable losses, power splitter losses and antenna gains are excluded for both models and for all sectors. We have assumed that the panel antennas are used matched to their specific environmental conditions in terms of horizontal and vertical beam widths. This way the antennas achieve the maximum gain. We have further assumed that the field strength that arrives at the mobile station can be compensated as the distance between the base

station and the mobile station increases. The carrier frequency is taken as $f = 2000$ *MHz*, so the wavelength, λ becomes 0.15 *m*. In the second part (Chapter 5) of the thesis; we have discussed radio network planning with related link budgets for different service types which are 12.2 *kbps* voice and 384 *kbps* real-time data (for vehicular in-car user) then comparing the cell ranges according to path loss models. We have used same measured data through the sectors which discussed in work part 1 (i.e. same morphology and topography correction factors, path loss formulations). In our calculation the standard deviation for log-normal fading is assumed to be equally affected and 8 *dB* for all sectors, so the fading margin is taken into account with this assumption during the simulation and calculation progress. And also we consider and compare specific high bandwidth services such as 12.2 *kbps* voice and 384 *kbps* real-time data therefore all related network planning concepts includes from our calculations. In 3GPP [14], performance tests for the mobile and base stations are defined in a propagation environment that operates under certain multipath propagation conditions. We have used the performance requirements of multipath fading case 3 (case 3 defines the multipath fading propagation condition that mobile user has 120 *Km/h* speed with heavy fading channels) which is determined by a maximum required block error rate as $<10^{-2}$. So in this thesis, radio network planning (also for radio link budget) implementation and simulation of both models are undertaken, assuming case 3 propagation conditions. For vehicular test environment, we need a channel impulse response model based on a tapped-delay line model which is given by 3GPP [10]. Since our propagation environment along the border lines form one sector to the

other has slowly changing structures, thus having a low small delay spread, we have employed the vehicular ‘Channel A’ model [10] in our calculations.

4.2 Path Loss Calculations

Path loss calculations have done separately for each sector with respect to both propagation models. Each propagation model defines its own calculation methods according to propagation condition on that environment. Extended Okumura Model mostly uses terrain level calculations but UMTS-Vehicular Model depends on building structure and building density.

4.2.1 Path Loss Calculation for Extended Okumura Model

The parameters affecting the path loss for Extended Okumura Model can be classified into three sub parts; effective antenna height, morphology correction and topographic correction. We have applied a suitable method to calculate these parameters independently for the sectors.

4.2.1.1 Effective Antenna Height Calculation

By applying the measured data from the Sector 1, 2 and 3 into the equations 2.5 and 2.6;

$$h_m = \frac{\sum_{i=0}^{90} h_i}{90+1}$$

With a distance of 2700 m from base station to mobile and a

resolution of 30 m, approximately 91 points are needed to obtain the following results for Sectors 1, 2 and 3 consecutively;

$$h_{m1} = 889.1 \text{ m}, h_n = 904.9 \text{ m}, h_{eff} = h_n - h_{m1} = 15.8 \text{ m} \text{ (Sector 1)}$$

$$h_{m2} = 855.8 \text{ m}, h_n = 904.9 \text{ m}, h_{eff} = h_n - h_{m2} = 49.1 \text{ m} \text{ (Sector 2)}$$

$$h_{m3} = 912.5 \text{ m}, h_n = 904.9 \text{ m}, h_{eff} = h_n - h_{m3} = -7.6 \text{ m} \text{ (Sector 3)}$$

The same method may be applied for distances of 6000 *m* from base station to mobile.

4.2.1.2 Morphology Correction Factor Calculation

By applying the procedure and the morphology type's assumptions (suburban, urban etc.) which explained in Chapter 2.3.1.2 into our terrains in all the sectors through to 2700 *m* (that is the distance between the base station and the mobile station), we obtain the following morphology correction factors.

$$C_m = -2.38 \text{ dB} \text{ (Sector 1)}$$

$$C_m = -4.31 \text{ dB} \text{ (Sector 2)}$$

$$C_m = -2.08 \text{ dB} \text{ (Sector 3)}$$

Note that our simulation implements the extension of the above calculations up to 6000 *m*.

4.2.1.3 Topographic Corrections Calculation

We have applied a suitable topographic correction method for each of the sectors, in our calculations we have used multiple knife-edge diffraction method for Sector 1 and clearance angle method for Sector 2 and 3. When we looked the measured topographic data through the sectors, it is seen that the for Sector 1 terrain shapes

include two main irregular and knife-edge hills that require multiple knife-edge diffraction method for topographic correction furthermore clearance angle method is useful for Sector 2 and Sector 3 because of terrain irregularity. In Sector 2, terrain height decreases slowly, and in Sector 3 terrain increases more steeply. So we have applied clearance angle method to find topographic correction through the terrain levels. The calculations given below are fixed for all sectors.

By setting $h_r = 1.5 \text{ m}$, $f = 2000 \text{ MHz}$, in equation 2.4, the following $c(h_r)$ is obtained, that is common to all sectors ;

$$c(h_r) = (1.1 \log_{10}(2000 \text{ MHz}) - 0.7) \times (1.5 \text{ m}) - (1.56 \log_{10}(2000 \text{ MHz}) - 0.8)$$

Hence; $c(h_r) = 0.05 \text{ dB}$.

4.2.1.4 Path Loss Calculation for Sector 1 Using Multiple Knife-Edge Diffraction Method

General profile for Sector 1 is shown in Figures 2.4 and 2.5. As seen from these figures, within a distance of 2000 m, terrain shapes include two main irregular and knife-edge hills named as M_1 and M_2 respectively. Since the verification requirements given in [8] are met, the calculation of the field strength could now be carried out by means of the knife-edge diffraction loss for Sector 1. From Figure 5;

$$H_{m1} = 14 \text{ m}, H_{m2} = 12 \text{ m}.$$

$$d = 2700 \text{ m}, \text{ for } d \gg H_t \Rightarrow x \approx d, \quad x = 2700 \text{ m}$$

$$a = 1265 \text{ m}, b = 565 \text{ m}, c = 870 \text{ m}, H_r = 1.5 \text{ m}, H_t = 8.9 \text{ m}$$

By inserting the numeric values given above parameters for H_{m1} , H_{m2} , d , x , a , b , c , H_r and H_t into the equations 2.7, 2.8 and 2.9; then h_1 , h_2 and h_3 are found as;

$$h_1 = 8.6 \text{ m}, \quad h_2 = 2.8 \text{ m}, \quad h_3 = 8.1 \text{ m}.$$

By applying equations 2.10, 2.11 and 2.12 for the obstacles M_1 and M_2 following results are obtained;

$$A_{m1} = 15.3 \text{ dB}, \quad A_{m2} = 11 \text{ dB}$$

Total topographic diffraction loss, C_d due to obstacles M_2 and M_1 found as from equation 2.13;

$$C_d = A_{m1} + A_{m2} \text{ then } C_d = 15.3 + 11 = 26.3 \text{ dB}$$

Next, we add this diffraction loss to the extended Okumura formulation as topographic correction factor. By using the results from Sections 4.2.1.1, 4.2.1.2 and 4.2.1.3 for Sector 1;

$$h_{eff} = 15.8 \text{ m}, \quad c(h_r) = 0.05 \text{ dB}$$

$$C_d = 26.3 \text{ dB}, \quad C_m = -2.38 \text{ dB}$$

Then the total path loss with correction factors from equation 2.3 is found to be;

$$L = 46.3 + 33.9 \log_{10}(2000 \text{ MHz}) - 13.82 \log_{10}(15.8 \text{ m}) - (0.05 \text{ dB}) + (44.9 - 6.55 \log_{10}(15.8 \text{ m})) \log_{10}(2.7 \text{ km}) - (-2.38 \text{ dB}) + (26.3 \text{ dB})$$

$$\text{Hence; } L = 186.4 \text{ dB}$$

4.2.1.5 Path Loss Calculation for Sector 2 Using Clearance Angle Method

The related terrain profile and its associated clearance angle perspective are shown in Figure 4.1 In this figure;

d is distance between transmitter and receiver (in m)

$h = h_n$ (physical height of the antenna above sea level) - h_r (mobile height) + horizontal line terrain height through the clearance angle path (in m)

φ is clearance angle (in $degree$)

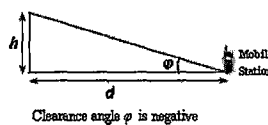
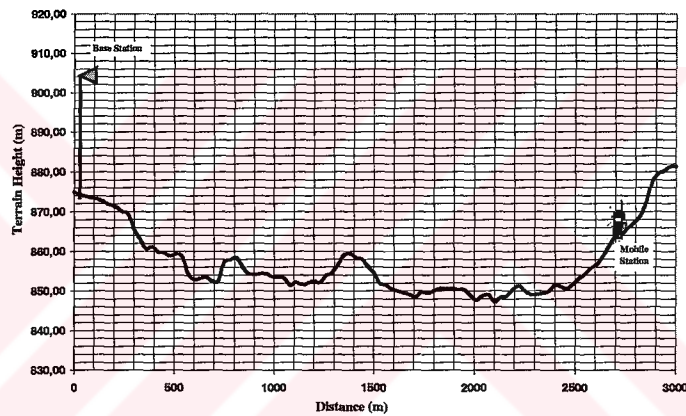


Figure 4.1: Terrain height profile for Sector 2

From Figure 4.1; $\tan(\varphi) = h / d = -0.0139$, $\varphi = -0.79^\circ$

By inserting the numeric values given above, into equations 2.14 and 2.15 the followings are obtained;

$$\Delta d = -0.84 \text{ dB}, \text{ and } C_d = -0.142 \text{ dB},$$

For Sector 2, by using the results of earlier sections; (4.2.1.1, 4.2.1.2 and 4.2.1.3)

$$h_{eff} = 49.1 \text{ m}, C_m = -4.31 \text{ dB}$$

Then by inserting the correction factors, the total path loss for this sector from equation 2.3 is found to be;

$$L = 46.3 + 33.9 \log_{10}(2000 \text{ MHz}) - 13.82 \log_{10}(49.1 \text{ m}) - (0.05 \text{ dB}) + \\ (44.9 - 6.55 \log_{10}(49.1 \text{ m})) \log_{10}(2.7 \text{ km}) - (-4.31 \text{ dB}) + (-0.142 \text{ dB})$$

$$\text{Hence; } L = 153.5 \text{ dB}$$

4.2.1.6 Path Loss Calculation for Sector 3 Using Clearance Angle Method

This calculation is based on the terrain profile of Sector 3 and the clearance angle perspective given in Figure 4.2. By substituting measured parameters;

$$\text{From Figure 4.2; } \tan(\varphi) = h / d = 0.0214, \varphi = 1.22^\circ,$$

Then from the equations 2.14 and 2.15

$$\Delta d = 20.8 \text{ dB} \quad \text{and} \quad C_d = 3.51 \text{ dB}$$

For Sector 3, by using the results of earlier sections; (4.2.1.1, 4.2.1.2 and 4.2.1.3)

$$h_{eff} = |-7.6| = 7.6 \text{ m}, C_m = -2.08 \text{ dB}$$

Then by inserting the correction factors, the total path loss for this sector from equation 2.3 is found to be;

$$L = 46.3 + 33.9 \log_{10}(2000 \text{MHz}) - 13.82 \log_{10}(7.6 \text{m}) - (0.05 \text{dB}) + (44.9 - 6.55 \log_{10}(7.6 \text{m})) \log_{10}(2.7 \text{km}) - (-2.08) + (3.51 \text{dB})$$

Hence; $L = 168.4 \text{ dB}$

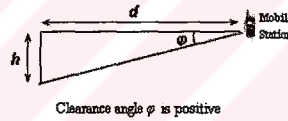
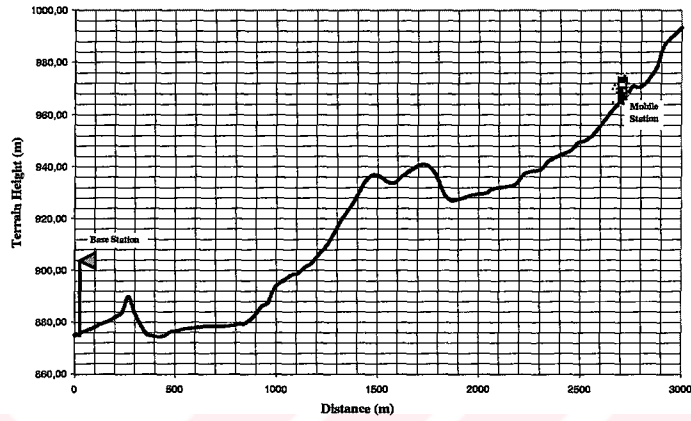


Figure 4.2: Terrain height profile for Sector 3

4.2.2 Path Loss Calculation for UMTS Vehicular Model

To find UMTS vehicular path losses for each sector we have used digital map and field measured data which collected from a particular site in Ankara. The collected data is given in the Table 4.1. By inserting the numerical values given in the Table 4.1 into the equation 2.1 independently for Sectors 1, 2 and 3, then total UMTS vehicular path losses are found as ;

$$L = 181.8 \text{ dB (Sector 1)}$$

$$L = 180.4 \text{ dB (Sector 2)}$$

$$L = 184.8 \text{ dB (Sector 3)}$$

Table 4.1: Measured results for UMTS vehicular model

Measured Parameters	Sector 1	Sector 2	Sector 3
$d(m)$	2700	2700	2700
$h_r(m)$	1.5	1.5	1.5
$x(m)$	15	15	15
$e(m)$	76.9	77	80.1
$H_t(m)$	30	30	30
$\Delta_m(m)$	14.4	13.3	17
$\Delta_{mr}(m)$	12.9	11.8	15.5
$\Delta_{hb}(m)$	15.5	16.6	12.9
$\Delta_{hm}(m)$	11.4	10.3	14
$r(m)$	18.8	18.2	20.8
$\Theta(\text{Degree})$	37.3 °	34.7 °	43 °

The following table summarizes the sample calculation of our path loss results at a distance of 2700 m from the base station for the two models studied.

Table 4.2: Path loss results for 2700 m

Propagation Model	Path Loss(dB) Sector 1	Path Loss(dB) Sector 2	Path Loss(dB) Sector 3
UMTS Vehicular	181.8	180.4	184.8
Extended Okumura	186.4	153.5	168.4

4.3 Results of Simulation Program

The implementation has been done in Matlab program. In the simulation program, topographic correction is added mainly according to the knife edge diffraction method for Sector 1 and by the clearance angle method for Sector 2 and Sector 3.

However in Sector 1 for a distance up to 1280 *m* and in the range between 2900 *m* and 3100 *m*, the terrain structure has sharp slopes. For these ranges we have applied clearance angle method and for the rest of the terrain up to 6000 *m*, knife edge diffraction method is used. When the simulation program is run using the measured morphology and topographic values, we obtain the respective plots given below. These graphs illustrate the path losses (in *dB* scale) with respect to the distance from the base station to mobile station on logarithmic scale. In these graphs, dashed lines show the path loss for UMTS vehicular model whereas solid lines refer to the path loss for extended Okumura covering the path lengths up to 6000 *m*. As expected, the graphs verify that the path loss will rise with increasing distances from the base station. From our simulation results and empirical formulations, we see that two factors play vital roles for the determination of path loss in UMTS vehicular method. These are explained below.

1) Average Building Height (Δ_{mr}): As may be detected from equation 2.1, this has a positive impact on path loss. This means that the increases in diffraction angle subtended at the mobile station lead to rising Δ_{mr} , which in turn causes L to increase.

2) Average Interbuilding Distance (ℓ): From equation 2.1, it is to be observed that interbuilding distance contributes inversely to path loss which means that L decreases with increasing ℓ

On the other hand, for extended Okumura method, when determining the path loss, three principal factors need to be taken into consideration.

-
- 1) Effective Antenna Height (h_{eff}): This is inversely proportional to terrain height, thus affecting the path loss likewise. That means as h_{eff} increases, path loss decreases.
 - 2) Topographic Correction Factor (C_d): This factor is directly proportional to terrain height. When the latter rises, causing the clearance angle to drop, path loss increases.
 - 3) Morphology Correction Factor (C_m): This factor reflects the morphological content of the environment. It adds in an ascending manner to path loss in the order of water, open area, park and forest, suburban and urban.

The following results are obtained by applying the two path loss models to all three sectors.

4.3.1 Sector 1

Within this sector, urbanization increases towards the inner and outer edges of the coverage area. Additionally terrain height increases up to a certain point 3100 m , afterwards decreases up to 3830 m and then past the point of 3830 m , it effectively remains flat. Other characteristics of this sector are that interbuilding distance decreases while building heights tend to increase as we get away from the base station. Figure 4.3 illustrates how these properties are reflected in both models and how they shape the individual curves for particular values of h_{eff} , C_m , C_d , ℓ and Δ_{mr} .

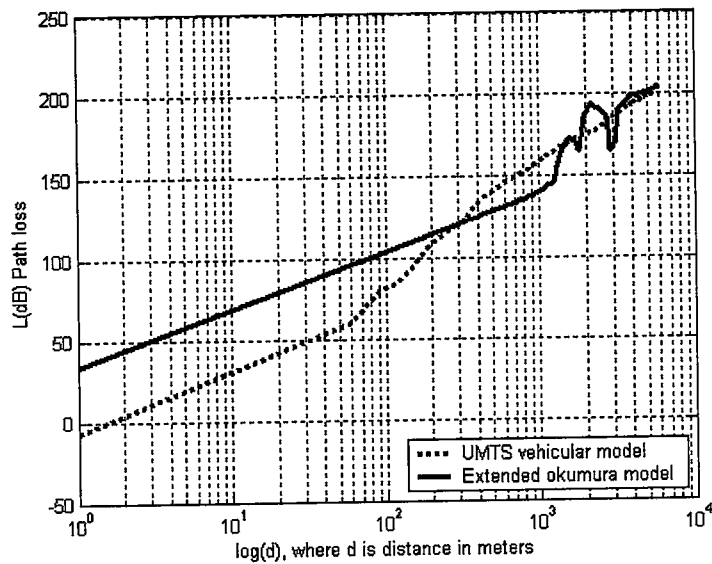


Figure 4.3: Path losses versus to distance (on log scale) for Sector 1

4.3.2 Sector 2

This sector develops towards open and park areas with increasing radial distance from the base station. Along the paths, we also see increases in average building height up to a certain distances (about 3480 m) then decreases here after and vice versa for interbuilding distances. Figure 4.4 shows how these properties are reflected in the application of both models in terms of h_{eff} , C_m , C_d , ℓ and Δ_{mr} .

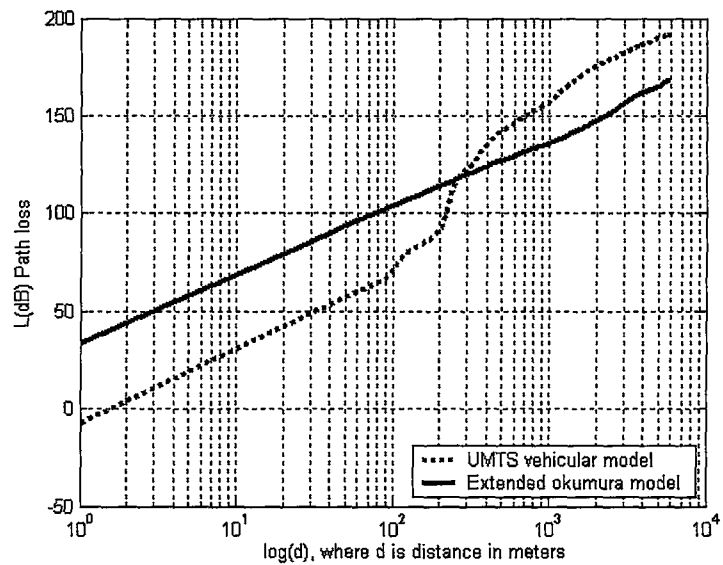


Figure 4.4: Path losses versus to distance (on log scale) for Sector 2

4.3.3 Sector 3

In this sector, morphology turns into suburban type with increasing distance from the base station, causing C_m also to increase. Additionally terrain height also increases along the same course causing C_d to increase. As a result for extended Okumura model that is more sensitive to topography, total path loss makes a peak around 2200 m. The individual behavior of both models is displayed in Figure 4.5.

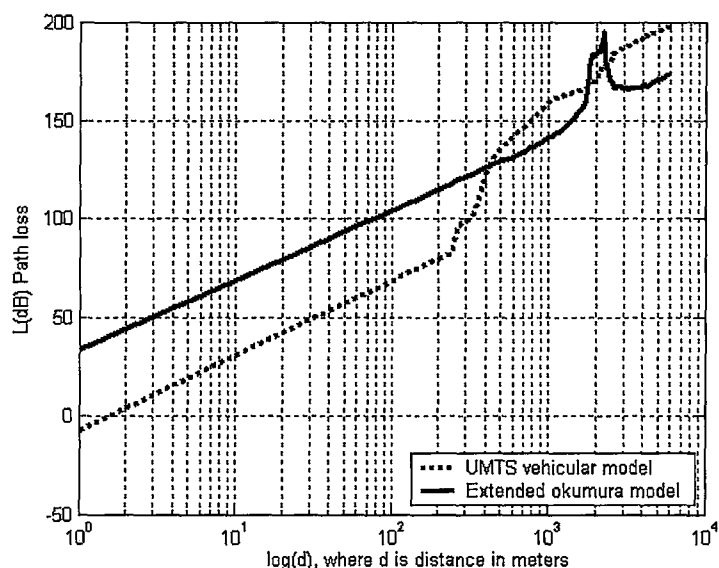


Figure 4.5: Path losses versus to distance (on log scale) for Sector 3

Examining the general behavior in graphs and related path loss equations, we conclude that the some parameters are more effective than the others. For instance in UMTS vehicular model, Δ_{mr} is more decisive than ℓ whereas in extended Okumura model is C_d more decisive than both h_{eff} and C_m . Looking at Figures 4.3, 4.4 and 4.5, we see that UMTS vehicular model is somewhat insensitive to terrain irregularities. Also it is seen that with in all sectors, the UMTS vehicular model predicts higher path loss values with respect to extended Okumura model that outside the high rise terrains and except for the range with in a few hundred meters distances from the base station, because with in these ranges there is not any buildings so the effect of the building density is nearly zero on UMTS model so we get lower path loss values for these ranges of calculations when we get away from the base station. Also we must remembered that these models are macro cellular models and developed to describe the radio characteristics of large areas and mostly

applicable for large distances from the base station so we had state on mostly the general behavior of path losses for long distances[1]. We may further state that the topographic structure of terrain is more effective than morphology structure of terrain in macro cellular extended Okumura model for any radio environments. It is evident from our results that we experience more path loss, as the morphology changes from open to park and suburban areas.



CHAPTER 5

RADIO LINK BUDGET CALCULATION

5.1 Radio Link Budget Calculation

In this part of the thesis, radio link budget calculation for two service types which are 12.2 *kbps* voice and 384 *kbps* real-time data (for vehicular A type channel in-car user) are made then a comparison of the cell ranges according to path loss (UMTS vehicular and extended Okumura) models is undertaken.

The assumptions used in the calculations of the link budgets for receivers and transmitters as follows;

(a) Max transmitter power; For voice service 21*dB*, for real-time data service 24 *dB*

(b) Mobile station gain is very small, so in radio link budget it is assumed as 0 *dB* for both services (real-time data and voice transmissions) and the value is fixed in the template.

(c) Cable, connector, and body losses (Transmitter); We have assumed as 3 *dB* for voice service and 0 *dB* for real-time data service. For real-time data services, we have assumed that mobile hand set is far away from user head so body loss will be too small, nearly 0 *dB*. [16]

(d) Transmitter equivalent isotropic radiated power (e.i.r.p.); By inserting the numerical values of row (a), row (b) and row (c) from radio link budget (which are given in the Tables 5.1 and 5.2) into the equation 3.1, e.i.r.p is found as:

$$d = 21 + 0 - 3 = 18dB \quad (\text{For voice service})$$

$$d = 24 + 0 - 0 = 24dB \quad (\text{For real-time data service})$$

(e) Thermal noise density (N_o); For outside temperature T we have assumed $12^\circ C = 285^\circ K$ for city of Ankara (which is taken by Turkish National Weather Administration's reports and shows the annual mean temperature of Ankara city). In radio link budget, thermal noise density as calculated above is taken into consideration equally for both services (real-time data and voice transmissions). By using the above assumption, in the equation 3.2, and after the conversion to dBm unit then the thermal noise density is found to be;

$$N_o = k \times T = 1.38 \times 10^{-23} \frac{Ws}{K} \times 285K = 3.93 \times 10^{-21} W / Hz$$

$$N_o = 10 \log_{10} \left(\frac{3.93 \times 10^{-21} W}{0.001W} \right) dBm / Hz \cong -174dBm / Hz$$

(f) Receiver noise figure (F); We have adopted 65deg18.4 sectored antenna (half-power horizontal beam width is 65° and the maximum receiver antenna gain is 18.4 dB), that is the antenna type generally used for 3 sectored macro cells. Also antenna temperature due to internal noise is $T_o = 24^\circ C = 297K$ for 65deg18.4 antennas [17]. By inserting these numeric values into the equation 3.3, then receiver noise figure is found to be;

$$F = 10 \log_{10} \left(1 + \frac{T_0}{T} \right) dB = 10 \log_{10} \left(1 + \frac{297 K}{285 K} \right) dB \cong 3.1 dB$$

In radio link budget, receiver noise figure is equally taken into account for both services (real-time data and voice transmission).

(g) Receiver noise density; By inserting the numerical values of row (e) and row (f) from radio link budget tables (Tables 5.1 and 5.2) into the equation 3.4, then receiver noise density is found to be:

$$g = -174 + 3.1 = 170.9 dB / Hz \text{ (Equal for both voice and real-time data services)}$$

(h) Receiver noise power; The value of B is constant for UMTS and equal to 3.84 Mhz and also defines the effective bandwidth of the system. By inserting the numerical values of T , F , B and k which are given in the calculation stage of row (e) and row (f) in radio link budget's fields (also seen from Tables 5.1 and 5.2) into the equation 3.5,

$$P_n = 1.38 \times 10^{-23} \frac{W_s}{K} \times 285 K \times 3.84 MHz \times 3.1 dB = 4.68 \times 10^{-14} W, \text{ and after the converting}$$

to dBm unit, noise power is found as;

$$P_n = 10 \log_{10} \left(\frac{4.68 \times 10^{-14} W}{1mW} \right) dBm = -103.3 dBm$$

(Same for voice and real-time data services)

(i) Interference margin; We have used maximum recommended uplink cell load to which a network should be planned is 70% and this leads from the equation 3.6, to

$\eta = -10 \log_{10}(1 - (70/100)) = 5.2dB$ of interference margin. (Equal for both voice and real-time data services)

(j) Receiver interference power; By inserting the numerical values of P_n and η which are calculated in the radio link budget's fields as row (h) and row (i) (also seen from Tables 5.1 and 5.2) into the equation 3.7,

$P_{RX} = 10^{(-103.3 + 5.2)/10} mW - 10^{-103.3/10} mW = 1.09 \times 10^{-10} mW$, and after the converting to dBm unit, interference power is found as:

$$P_{RX} = 10 \log_{10} \left(\frac{1.09 \times 10^{-10} mW}{1mW} \right) dBm = -99.6dBm .$$

This value is fixed and equal in the link budget for voice and real-time data services.

(k) Total effective noise power; By inserting the numerical values of P_n and P_{RX} which are calculated in the radio link budget's fields as row (h) and row (j) (also seen from Tables 5.1 and 5.2) into the equation 3.8.

$$P_{NP} = 10^{(-103.3/10)} mW + 10^{(-99.6/10)} mW = 1.56 \times 10^{-10} mW ,$$

and after the converting to dBm unit, Total effective noise power is found as:

$$P_{NP} = 10 \log_{10} \left(\frac{1.56 \times 10^{-10} mW}{1mW} \right) dBm = -98.1dBm$$

(l) Processing gain; In our case bit rate of voice data transmission is 12.2 *kbps* and the bit rate of real-time data is 384 *kbps*. The value of B is constant for UMTS and

can be defined in terms of $Mcps$ unit which equals to $3.84 Mcps$. By inserting the numerical values of W , B given the above into equation 3.9 independently for voice and real-time data, the processing gains are found as;

$$PG = 10 \log_{10} \left(\frac{3.84 Mcps}{12.2 kcps} \right) = 24.9 dB \quad (\text{For voice service})$$

$$PG = 10 \log_{10} \left(\frac{3.84 Mcps}{384 kcps} \right) = 10.0 dB \quad (\text{For real-time data service})$$

(m) Required E_b/N_o ; We have used the performance requirements of multipath fading case 3 (case 3 defines the multipath fading propagation condition that mobile user has $120 Km/h$ speed with heavy fading channels) which is determined by a maximum required block error rate as $<10^{-2}$. Then, for received E_b/N_o ratio of service channels with related BLER of 10^{-2} are given as [9]:

$$E_b/N_o = 7.2 dB \quad (\text{For voice service})$$

$$E_b/N_o = 3.6 dB \quad (\text{For real-time data service})$$

(n) Receiver sensitivity; By inserting the numerical values of m , l and k which are calculated in the radio link budget's fields as row (m), row (l) and row (k) (which are given in the Tables 5.1 and 5.2) into the equation 3.10 then receivers sensitivities are found as:

$$n = 7.2 - 24.9 + (-98.1) = -115.8 dB \quad (\text{For voice service})$$

$$n = 3.6 - 10.0 + (-98.1) = -104.5 dB \quad (\text{For real-time data service})$$

(o) Receiver antenna gain; A 65deg18.4 sectored antenna (half-power horizontal beam width is 65° and the maximum receiver antenna gain is 18.4 dB) is assumed that is the antenna type generally employed for 3 sectored macro cells for UMTS applications [13]. This way we obtain the maximum receiver antenna gain of 18.4 dB for both services (real-time data and voice transmission) [17].

(p) Cable, connector losses (Receiver); The value is fixed in the link budget calculations and taken as 2 dB for 65deg18.4 sectored antennas [13]. This loss value is taken to be equal for each radio link budget on both services (real-time data and voice transmission).

(r) Maximum path loss; By inserting the numerical values of d , n , o and p which are calculated in the radio link budget's fields as row (d), row (n), row (o) and row (p) (given in the Tables 5.1 and 5.2) into the equation 3.11, the respective maximum path lose values are found as:

$$r = 18 - (-115.8) + 18.4 - 2 = 150.2 \text{ dB} \quad (\text{For voice service})$$

$$r = 24 - (-104.5) + 18.4 - 2 = 144.8 \text{ dB} \quad (\text{For real-time data service})$$

(s) Log-normal fade margin; In our link assumption, outage probability is set to %10 which means that link has to have adequate power ninety percent of the time for points on the cell edge, then $P_{out} = 0.1$, and from the equation 3.12, $(\rho / \sigma) \approx 1.29$, or $\rho = 1.29\sigma$. For $\sigma = 8 \text{ dB}$ (standard deviation for the log-normal fading in urban areas is stated to be around 8 dB [10]), $\rho = 10.3 \text{ dB}$. This is the additional log-

normal fading margin required to maintain the link at ninety percent of the points along edge of a cell for this specific case.

(*t*) In-car loss; According to measurements, the matter loss of a car approximately is 4-7 *dB*. So in our link budget, we have assumed in-car loss to be 4 *dB* for both services (voice and real-time data).

(*u*) Allowed propagation loss for cell range; By inserting the numerical values of *r*, *s* and *t* which are calculated in the radio link budget's fields as row (*r*), row (*s*) and row (*t*) (given in the Tables 5.1 and 5.2) into the equation 3.14, then permitted propagation path losses are found as:

$$u = 150.2 - 10.3 - 4.0 = 135.9 \text{ dB} \quad (\text{for voice service})$$

$$u = 144.8 - 10.3 - 4 = 130.5 \text{ dB} \quad (\text{for real-time data service})$$

Calculated results of radio link budgets for two types of services (12.2 *kbps* voice and 384 *kbps* real-time data) are given in the Tables 5.1 and 5.2.

Table 5.1: Link budget of 12.2 *kbps* voice service (120 km/h, in-car users)

Transmitter (mobile)		
(a)	Maximum transmitter power (in <i>dBm</i>)	21.0
(b)	Mobile antenna gain (in <i>dB</i>)	0.0
(c)	Cable, connector and body loss (in <i>dB</i>)	3.0
(d)	Transmitter equivalent isotropic radiated power (in <i>dBm</i>)	18.0
Receiver (base station)		
(e)	Thermal noise density (in <i>dBm/Hz</i>)	-174.0
(f)	Receiver noise figure (in <i>dB</i>)	3.1
(g)	Receiver noise density (in <i>dBm/Hz</i>)	-170.9
(h)	Receiver noise power (in <i>dBm</i>)	-103.3
(i)	Interference margin (in <i>dB</i>)	5.2
(j)	Receiver interference power (in <i>dBm</i>)	-99.6
(k)	Total effective noise power (in <i>dBm</i>)	-98.1
(l)	Processing gain (in <i>dB</i>)	24.9
(m)	Required E_b/N_o (in <i>dB</i>)	7.2
(n)	Receiver sensitivity (in <i>dBm</i>)	-115.8
(o)	Receiver antenna gain (in <i>dB</i>)	18.4
(p)	Cable and connector losses (in <i>dB</i>)	2.0
(r)	Maximum path loss (in <i>dB</i>)	150.2
(s)	Log-normal fade margin (in <i>dB</i>)	10.3
(t)	In-car loss (in <i>dB</i>)	4.0
(u)	Allowed propagation loss for cell range (in <i>dB</i>)	135.9

Table 5.2: Link budget of 384 *kbps* real-time data service (120 km/h, in-car users)

Transmitter (mobile)		
(a)	Maximum transmitter power (in <i>dBm</i>)	24.0
(b)	Mobile antenna gain (in <i>dB</i>)	0.0
(c)	Cable, connector and body loss (in <i>dB</i>)	0.0
(d)	Transmitter equivalent isotropic radiated power (in <i>dBm</i>)	24.0
Receiver (base station)		
(e)	Thermal noise density (in <i>dBm/Hz</i>)	-174.0
(f)	Receiver noise figure (in <i>dB</i>)	3.1
(g)	Receiver noise density (in <i>dBm/Hz</i>)	-170.9
(h)	Receiver noise power (in <i>dBm</i>)	-103.3
(i)	Interference margin (in <i>dB</i>)	5.2
(j)	Receiver interference power (in <i>dBm</i>)	-99.6
(k)	Total effective noise power (in <i>dBm</i>)	-98.1
(l)	Processing gain (in <i>dB</i>)	10.0
(m)	Required E_b/N_o (in <i>dB</i>)	3.6
(n)	Receiver sensitivity (in <i>dBm</i>)	-104.5
(o)	Receiver antenna gain (in <i>dB</i>)	18.4
(p)	Cable and connector losses (in <i>dB</i>)	2.0
(r)	Maximum path loss (in <i>dB</i>)	144.8
(s)	Log-normal fade margin (in <i>dB</i>)	10.3
(t)	In-car loss (in <i>dB</i>)	4.0
(u)	Allowed propagation loss for cell range (in <i>dB</i>)	130.5

5.2 Cell Range Calculation

Now we apply budget calculations to propagation models to find maximum cell ranges. From Tables 5.1 and 5.2 (as row (u)) maximum allowable path losses have been found as;

$L = 135.9$ dB (For voice service), $L = 130.5$ dB (For real-time data service)

Then we apply two (12.2 *kbps* voice and 384 *kbps* real-time data) types of services to each propagation model (extended Okumura and UMTS vehicular) to find the maximum allowed cell ranges; To find the cell ranges, we have used the area morphology types, topography types and building structures that are the same as those in Chapter 4. A three sector structure is taken, and then by inserting the mean values of measurements for these three sectors into computer simulation we observe the following cell ranges for each path loss model. The parameters in this simulation are calculated from the approximation method which allows us to find cell range for unknown roots of the path loss equations. Measured values of the parameters (which are given below) used in the equations 2.1 and 2.3, satisfy the maximum allowable path loss for the cell ranges.

From radio link budget calculations for 12.2 *kbps* voice service, we know that the maximum allowable path loss is 135.9 *dB*; then inserting the following values; $A_{hb} = 24.2$ *m*, $H_t = 30$ *m*, $\ell = 97.7$ *m*, $\Theta = 10.3^\circ$, $L = 135.9$ *dB*, $r = 15.28$ *m*, $\lambda = 0.15$ *m* in to the equation 2.1(UMTS vehicular model) for 12.2 *kbps* voice service, the max cell range is found as; $d = 470$ *m*

$L = 135.9 \text{ dB}$, $C_m = -1.776$, $c(h_r) = 0.05$, $h_{\text{eff}} = 33.13 \text{ m}$, $h_r = 1.5 \text{ m}$, $f = 2000 \text{ Mhz}$,

$C_d = 0.227$

Using the values in equation 2.3 (extended Okumura model) for 12.2 *kbps* voice service, the max cell range is found as; $d = 812 \text{ m}$

From radio link budget calculation for 384 *kbps* real-time data service, we know that the max allowable path loss is 130.5 *dB*.

Using the numeric values; $\Delta_{hb} = 25.4 \text{ m}$, $H_t = 30 \text{ m}$, $\ell = 100.5 \text{ m}$, $\Theta = 7.80^\circ$, $L = 130.5 \text{ dB}$, $r = 15.12 \text{ m}$, $\lambda = 0.15 \text{ m}$ in equation 2.1(UMTS vehicular model) for 384 *kbps* real-time data service, the max cell range is found as; $d = 407 \text{ m}$

$L = 130.5 \text{ dB}$, $C_m = -1.80$, $c(h_r) = 0.05$, $h_{\text{eff}} = 32.3 \text{ m}$, $h_r = 1.5 \text{ m}$, $f = 2000 \text{ Mhz}$, $C_d = 0.09$

Using the numeric values; in the equation 2.3 (extended Okumura model) for 384 *kbps* real-time data service, the max cell range is found as; $d = 568 \text{ m}$

The results of these calculations for both propagation models are given in the Table 5.3.

Table 5.3: Cell ranges with respect to service type

Propagation Model	Cell Range (m)	
	12.2 <i>Kbps</i> voice	384 <i>kbps</i> real-time data
UMTS Vehicular	470 <i>m</i>	407 <i>m</i>
Extended Okumura	812 <i>m</i>	568 <i>m</i>

In radio link budget calculation, we have used a three sectored cell site, so $K = 1.95$ for both voice service and real-time data service, then applying results given in the Table 5.3 to equation 3.16, the radius of hexagonal shaped cell found as;

For 12.2 *kbps* voice service;

$$D = \sqrt{\frac{2 \times 1.95 \times 812^2}{3\sqrt{3}}} = 703.5m \text{ (extended Okumura model)}$$

$$D = \sqrt{\frac{2 \times 1.95 \times 470^2}{3\sqrt{3}}} = 407.2m \text{ (UMTS vehicular model)}$$

For 384 *kbps* real-time data service;

$$D = \sqrt{\frac{2 \times 1.95 \times 568^2}{3\sqrt{3}}} = 492.1m \text{ (extended Okumura model)}$$

$$D = \sqrt{\frac{2 \times 1.95 \times 407^2}{3\sqrt{3}}} = 352.6m \text{ (UMTS vehicular model)}$$

In order to obtain the hexagonal shaped cells, we have used a computer simulation model applicable to both link budgets (for 12.2 *kbps* voice and 384 *kbps* real-time data) and both propagation models (extended Okumura and UMTS vehicular models). After running the simulation program, we are observed the results given in the Figure 5.1 and Figure 5.2. Figure 5.1 shows the hexagonal shaped cells of 12.2 *kbps* voice service for both propagation models and Figure 5.2 shows the hexagonal shaped cells of 384 *kbps* real-time data service for both propagation models.

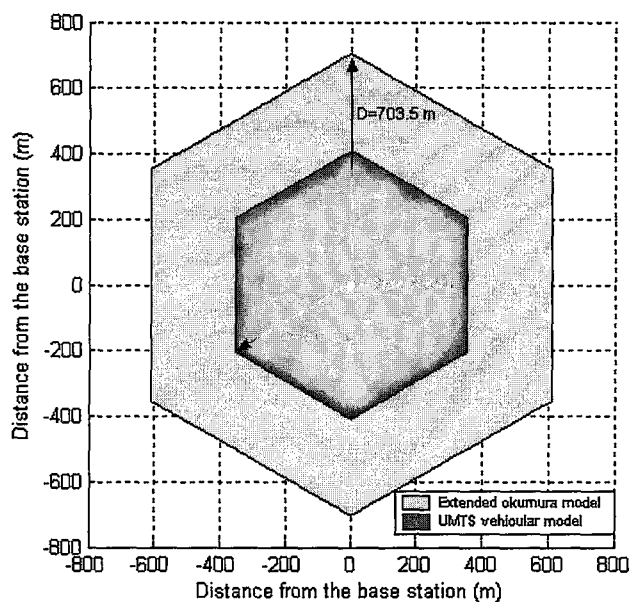


Figure 5.1: Cell structures for 12.2 kbps voice

It is seen from the cell structures that UMTS vehicular model predicts shorter cell ranges in comparison to extended Okumura model. Since we already know from the

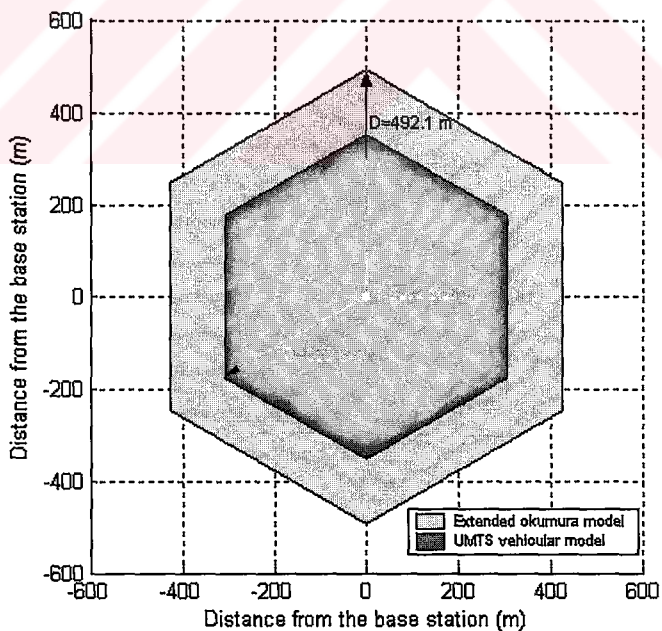


Figure 5.2: Cell structures for 384 kbps real-time data

findings of Chapter 4 that the diffraction from the buildings has greater impact on path losses than other effects such as morphologic and topographic structure of the terrain. Since the topographic and morphologic terrain structure was not so undulated in the measurement area, the cell range decreased and path loss increased (see equations 2.1 and 2.3). The building density is also increased due to this effect we obtain smaller cell range for UMTS propagation model than extended Okumura model. These results are in agreement with path loss figures of the two propagation models found in Chapter 4.



CHAPTER 6

CONCLUSIONS

In this thesis, for specific environments, we have investigated the propagation prediction ability of UMTS vehicular ITU-R and extended Okumura Hata models. Comparison of two macro cellular methods is made via simulation. Numerical evaluations are made under the conditions of various types of vegetation, morphology and terrain heights. The results show that for UMTS vehicular model, path loss model is affected mostly by average building height (Δ_{mr}), whereas for extended Okumura model, path loss are affected mostly by topographic structure of the terrain (C_d) and effective antenna height (h_{eff}). It is noted that UMTS vehicular path loss model generally predicts higher path loss values than the extended Okumura model except for regions of extremely hilly terrains. Our findings indicate that diffraction from the buildings has a greater impact on path losses than the other effects such as morphologic and topographic structure of the terrain. We have also observed that for different service types such as 12.2 *kbps* voice and 384 *kbps* real-time data, UMTS vehicular ITU-R model predicts shorter cell ranges in comparison to extended Okumura Hata model. Our results show that UMTS vehicular ITU-R model mostly depended to building density between the base station and mobile station but extended Okumura Hata model effected heavily from the topographic

and morphologic structure of the terrain on that radio propagation environment, so to calculate the cell ranges for the region in the city center or in suburban areas for radio network planning, UMTS vehicular ITU-R model gives the acceptable cell ranges with respect to extended Okumura Hata model, but in the rural areas it will be suitable for using the extended Okumura Hata model in radio link budget. Furthermore, it is important for a UMTS network to selection of radio propagation model according to vegetation because, that affects cell range of base station. So the optimum cell range effects cost of investment on radio network planning for UMTS operators. In our country 3rd generation technology will have a great impact on telecommunication industry in near future, so this work can be considered as a basis on development path on demands for designing a UMTS network.

REFERENCES

- [1] ITU Recommendation, "Guidelines for Evaluation of Radio Transmission Technologies for IMT-2000" ITU-R M.1225, 1997.
- [2] Hata, M. "Empirical Formula for Propagation Loss in Land Mobile Radio Service" IEEE Trans. Vehicular Technology. Vol. 29, No. 3, 1980.
- [3] COST-231, "Urban Transmission Loss Models for Mobile Radio in the 900- and 1800 MHz Bands (revision 2)" COST 231 TD (90) rev. 1, 1991.
- [4] Recommendations and Reports of the CCIR, Vol. 5, 1986.
- [5] Deygout, J. "Multiple Knife-edge Diffraction of Microwaves, IEEE Trans. Antennas and Propagation" Vol. AP-14, No. 4, 1966.
- [6] ITU Recommendation, "VHF and UHF propagation curves for the frequency range from 30 MHz to 1 000 MHz Broadcasting services" ITU-R P.370-7, 1995.
- [7] CCIR Study Groups Period 1978-1982 European Broadcasting Union, "Improvement of Predictions of Field Strengths in VHF and UHF Bands," Doc. 5/28-E, 1980.
- [8] CCIR, "17th Plenary Assembly, Düsseldorf" Rep. 5673, Rec. 3704, Vol. 5, 1990.
- [9] 3GPP, TSG RAN, "Radio Transmission and reception for UMTS" TR 125.102, version 5.0.1, 1998.

- [10] 3GPP, TSG RAN, "Selection Procedures for the Choice of Radio Transmission Technologies for UMTS" TR 101.112, Version 3.2.0, 1998.
- [11] J.Lempiainen, M. Manninen "Radio Interface System Planning for GSM, GPRS, UMTS", Kluwer Academic Publishers, 2001.
- [12] ITU Recommendation, "Radio Noise" ITU-R P.214.3., 1998.
- [13] J.Laiho, A. Wacker, "Radio network planning and optimization for UMTS", John Wiley & Sons, 2001.
- [14] 3GPP, TSG RAN, "UE Radio Transmission and Reception (FDD)" TS 3G 25.104, Version 3.7.0, 1998.
- [15] K. H. Kim. "Handbook of CDMA System Design, Engineering, and Optimization" Prentice Hall, 2000,
- [16] H.Holma, A. Toskala, "WCDMA for UMTS", John Wiley & Sons, 2001.
- [17] Engineering catalog for PCS panels, from http://www.kathrein-scala.com/pcs-umts_panel.php, 2004